Table S1. A summary of rBC size distribution parameters for the 14 emission flights, including MMD (mass median diameter; in nm), $Width_{mass}$ (mass distribution width; dimensionless), NMD (number median diameter; in nm), and $Width_{number}$ (number distribution width; dimensionless).

Date (flight ID)	MMD	$Width_{mass}$	NMD	$Width_{number}$
14 August, 2013 (F_8/14)	153.75 ± 0.64	0.71 ± 0.01	76.18 ± 0.64	0.67 ± 0.01
15 August, 2013 (F_8/15)	144.82 ± 0.54	0.74 ± 0.01	66.99 ± 0.44	0.71 ± 0.01
17 August, 2013 (F_8/17)	145.70 ± 1.57	0.72 ± 0.02	66.61 ± 1.33	0.73 ± 0.02
19 August, 2013 (F_8/19)	141.82 ± 0.58	0.75 ± 0.01	61.12 ± 0.65	0.75 ± 0.01
20 August, 2013 (F_8/20)	134.46 ± 0.99	0.74 ± 0.02	62.18 ± 0.80	0.72 ± 0.01
21 August, 2013 (F_8/21)	136.19 ± 0.67	0.70 ± 0.01	63.99 ± 0.69	0.72 ± 0.01
22 August, 2013 (F_8/22)	141.98 ± 0.98	0.70 ± 0.01	64.35 ± 1.16	0.74 ± 0.01
24 August, 2013 (F_8/24)	135.46 ± 0.94	0.74 ± 0.02	63.14 ± 0.56	0.71 ± 0.01
26 August, 2013 (F_8/26)	135.02 ± 0.37	0.61 ± 0.01	78.38 ± 0.54	0.61 ± 0.01
28 August, 2013 (F_8/28)	138.82 ± 0.71	0.74 ± 0.01	63.77 ± 0.41	0.72 ± 0.00
29 August, 2013 (F_8/29)	134.00 ± 0.46	0.70 ± 0.01	64.65 ± 0.48	0.70 ± 0.01
2 September, 2013 (F_9/2)	135.78 ± 2.04	0.72 ± 0.03	63.71 ± 1.13	0.71 ± 0.01
3 September, 2013 (F_9/3)	137.53 ± 0.93	0.76 ± 0.02	64.64 ± 0.70	0.70 ± 0.01
6 September, 2013 (F_9/6)	135.01 ± 0.77	0.71 ± 0.01	66.00 ± 0.71	0.69 ± 0.01

Table S2. A summary of rBC size distribution parameters for the 3 transformation flights. Results from successive flight screens are shown separately for each flight.

Flight and screen ID	MMD	$Width_{mass}$	NMD	$Width_{number}$
4 September, 2013 (F_9/4)				
Screen #1	140.87 ± 0.43	0.70 ± 0.01	69.07 ± 0.36	0.69 ± 0.00
Screen #2	141.13 ± 0.88	0.71 ± 0.01	71.59 ± 0.62	0.67 ± 0.01
Screen #3	147.47 ± 1.45	0.74 ± 0.02	71.11 ± 0.95	0.69 ± 0.01
Screen #4	146.97 ± 2.71	0.76 ± 0.04	71.11 ± 0.89	0.68 ± 0.01
Screen #5	142.42 ± 0.60	0.68 ± 0.01	72.00 ± 0.47	0.67 ± 0.01
19 August, 2013 (F_8/19)				
Screen #1	139.76 ± 1.67	0.76 ± 0.03	58.21 ± 2.26	0.77 ± 0.03
Screen #2	139.33 ± 1.78	0.74 ± 0.03	63.33 ± 2.04	0.73 ± 0.02
Screen #3	145.12 ± 1.57	0.79 ± 0.02	59.33 ± 2.29	0.78 ± 0.03
5 September, 2013 (F_9/5)				
Screen #1	149.85 ± 2.46	0.74 ± 0.03	70.88 ± 1.23	0.70 ± 0.02
Screen #2	148.79 ± 1.19	0.67 ± 0.02	72.67 ± 0.92	0.70 ± 0.01
Screen #3	151.62 ± 1.54	0.71 ± 0.02	73.48 ± 1.51	0.70 ± 0.02

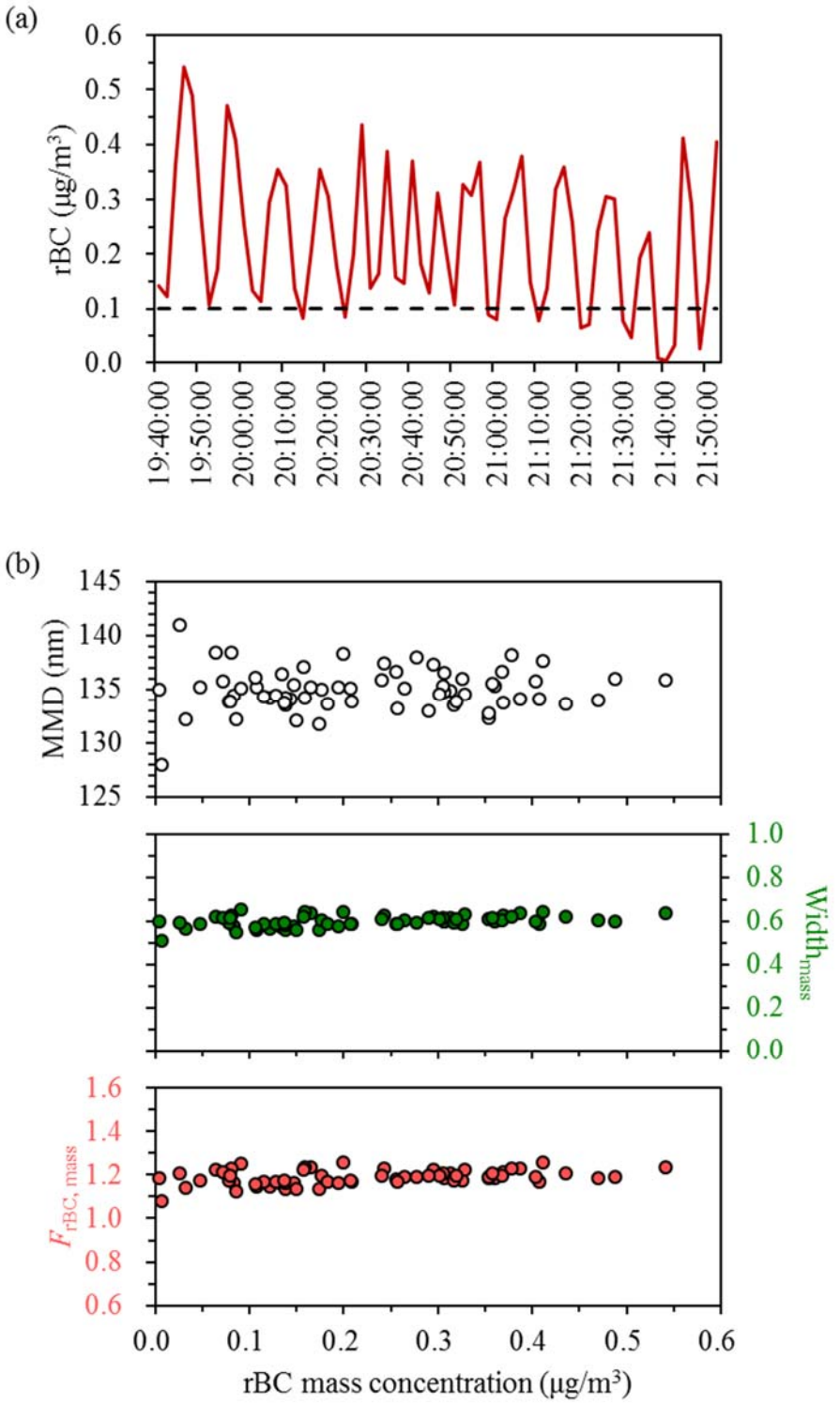

Figure S1. (a) Temporal variation of 2-min averaged rBC mass concentration during F_8/26, and **(b)** dependences of rBC MMD, $Width_{mass}$ and $F_{rBC,\,mass}$ on rBC concentration. The dashed line in (a) indicates an rBC concentration of 0.1 μg/m^3 which can be used to distinguish the typical in- and out-of-plume conditions for this flight.

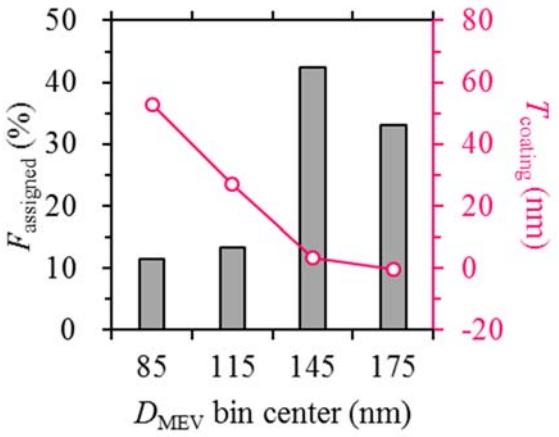

Figure S2. Dependences of coating thickness ($T_{coating}$) and the fraction of rBC cores that can be assigned a coating thickness ($F_{assigned}$, in %) on rBC core size (D_{MEV}) for the emission flight F_9/3. Refer to the caption of Figure 10 in the main manuscript for more details.

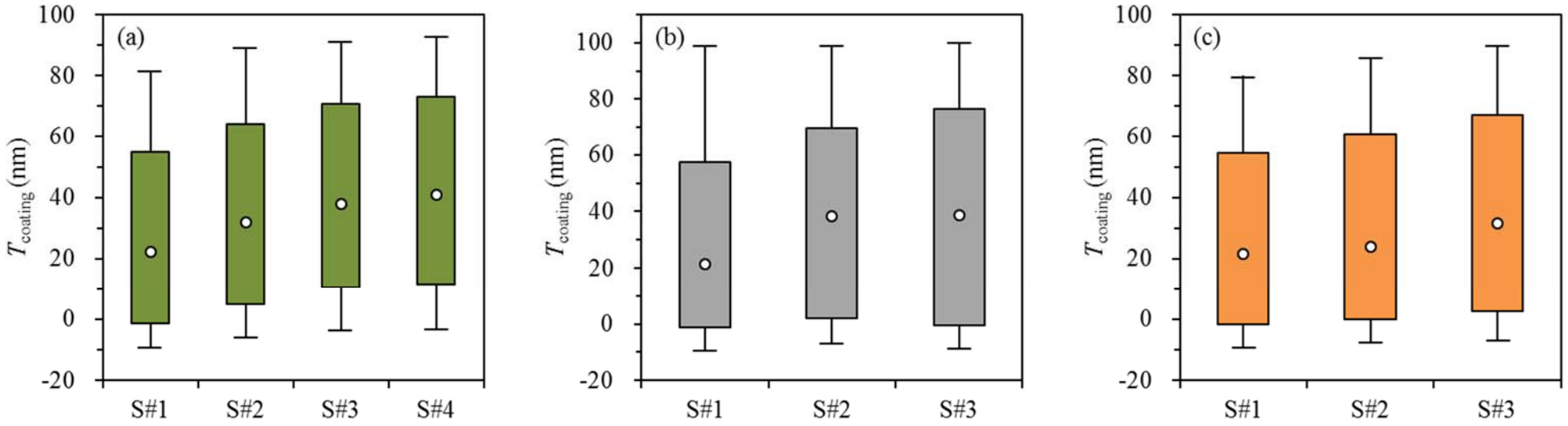

Figure S3. Evolutions of in-plume coating thickness ($T_{coating}$) for rBC cores in the D_{MEV} range of 130−160 nm during the transformation flights **(a)** F_9/4, **(b)** F_8/19 and **(c)** F_9/5. The counts of the 130−160 nm rBC cores that can be assigned a coating thickness are ~ 2450−3600, 300−400, and 700−1600 for successive flight screens of F_9/4, F_8/19 and F_9/5, respectively. $F_{assigned}$ are ~ 35−45%, 30−35%, and 30−45% for the 130−160 nm rBC cores observed during F_9/4, F_8/19 and F_9/5, respectively.